J Solid State Electrochem (2004) 8: 611–617
DOI 10.1007/s10008-003-0489-2

ORIGINAL PAPER

Stefan Diethelm · Joseph Sfeir · Frank Clemens
Jan Van herle · Daniel Favrat

Planar and tubular perovskite-type membrane reactors for the partial oxidation of methane to syngas

Received: 11 April 2003 / Accepted: 29 September 2003 / Published online: 4 March 2004

Abstract Dense planar and tubular oxygen separation membranes of $La_{0.6}Ca_{0.4}Fe_{0.75}Co_{0.25}O_{3-\delta}$ were investigated as reactors for the partial oxidation (POX) of methane to syngas. Their permeation properties were measured in an air/argon pO_2 gradient as a function of temperature. At 900 °C, the oxygen flux through a 1.26-mm-thick membrane was 0.075 μmol/cm^2·s and through a 0.25-mm-thick tube, 0.24 μmol/cm^2·s.

For the POX measurements, a catalyst was added to the membrane and methane was introduced on the argon side. This resulted in a gradual increase of the oxygen flux with increasing concentration of methane, reaching 2 μmol/cm^2·s at 900 °C with pure methane. For the planar reactor, the CO selectivity reached 99% and the CH_4 conversion 75% at 918 °C with pure methane. For the tubular reactor, the CO selectivity and CH_4 conversion were 83 and 99%, respectively, under the same conditions. After 1,400 h of operation in a tubular POX reactor, the membrane was examined revealing phase demixing and local decomposition.

Keywords $La_{0.6}Ca_{0.4}Fe_{0.75}Co_{0.25}O_{3-\delta}$ · Oxygen separation membrane · Extrusion · Kinetic demixing · Syngas

Presented at the OSSEP Workshop "Ionic and Mixed Conductors: Methods and Processes", Aveiro, Portugal, 10–12 April 2003

S. Diethelm (✉) · J. Van herle · D. Favrat
Laboratory for Industrial Energy Systems (LENI), STI,
Swiss Federal Institute of Technology, 1015 Lausanne,
Switzerland
E-mail: stefan.diethelm@epfl.ch
Tel.: +41-21-693-5968
Fax: +41-21-693-3502

J. Sfeir
HTceramix, EPFL Science Park, PSE-A,
1015 Lausanne, Switzerland

F. Clemens
Swiss Federal Laboratory for Materials Testing and Research
(EMPA), 8600 Dübendorf, Switzerland

Introduction

Over the last decade, mixed conducting perovskites have been thoroughly investigated as membrane materials for high-temperature oxygen separation [1]. Such membranes can advantageously be integrated in chemical processes requiring pure oxygen [2], such as the partial oxidation (POX) of methane to synthesis gas (syngas) [3]. Syngas is the principal feedstock for gas-to-liquid (GTL) processes based on Fischer–Tropsch and methanol synthesis, which are of growing interest for both economical and environmental reasons [4, 5]. It is also the intermediate in the production of hydrogen, ammonia, ethylene and other base chemicals. Furthermore, this hydrogen-rich gas mixture can be directly converted into electricity by solid oxide fuel cell (SOFC) systems. Combining oxygen separation and reaction in a single unit, as in a membrane-based POX reactor, is expected to cut the cost of syngas production by 25–35% from present production methods [4].

The concept of a POX reactor based on an oxygen separation membrane was initially demonstrated in 1992 by Balachandran et al. [6]. Since then, much effort has been devoted to this field with more or less success [7, 8, 9, 10, 11, 12]. In particular, two important consortia of companies, led respectively by*Praxair Inc.*and *Air Products and Chemicals Inc.*, were created for the development of such reactors.

The critical issue of this technology is mainly the stability of the membrane material subject to very harsh operating conditions, being exposed to air on one side and methane on the other. Failures during operation were reported and explained by development of internal stresses due to an inhomogeneous chemical expansion of the material across the membrane [13, 14]. Local decomposition of the material exposed to methane was also invoked as a possible fracture cause [13]. Kinetic demixing or decomposition of the membrane material in a strong oxygen chemical potential gradient was observed [15] as well as surface segregation and decomposition [8].

In this study we examine the performance and stability of $La_{0.6}Ca_{0.4}Fe_{0.75}Co_{0.25}O_{3-\delta}$ membranes for oxygen separation in a POX reactor. Two designs were considered for this application: planar and tubular. The performances of both types of reactor are analysed and compared. The membranes were examined after operation to evaluate the stability of this compound under real operating conditions.

Experimental

Powder synthesis

The $La_{0.6}Ca_{0.4}Fe_{0.75}Co_{0.25}O_{3-\delta}$ powder was produced by the solid-state reaction route. Iron oxide (Fluka, Switzerland) and cobalt oxide (Auer-Remy, Germany) powders were first ball-milled in an aqueous solution with an organic processing aid. After milling, lanthanum hydroxide and calcium carbonate (Fluka, Switzerland) were added and the resulting slurry was spray dried and sintered at 1,250 °C. The powder was then ball-milled a second time in order to get an average particle size of 2 μm. The phase purity was checked by X-ray diffraction.

Sample preparation

The disc-shaped pellet was prepared by uniaxial compaction of the powder at 100 MPa and sintered in air at 1,300 °C for 4 h.

For the tube fabrication, the powder was mixed with a commercial wax mixture and polyethylene in a roller-blade high-shear mixer (torque rheometer Rheomix 3000, Thermo Haake Gebrüder Haake GmbH) between 130 and 170 °C. The optimal ceramic volume fraction was 53%. Tubes were extruded with a single screw extruder (Rheomex 202, Thermo Haake Gebrüder Haake GmbH) and a die (outer diameter: 6 mm, inner diameter: 4.9 mm). The tubes were then sintered on V-shaped Al_2O_3supports at 1,300 °C for 4 h, with a prior debinding plateau.

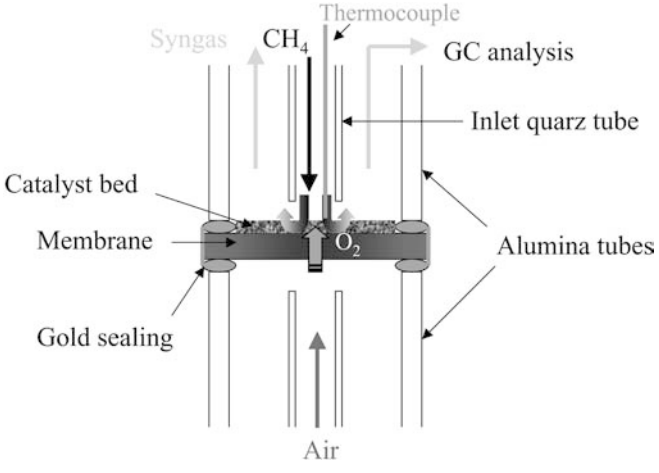

Fig. 1 Planar reactor design used for the partial oxidation of methane to syngas

Reactor designs

Planar

The design of the planar reactor is shown in Fig. 1. A 24-mm-diameter pellet was clamped between two Al_2O_3 tubes using gold-ring joints for sealing. The cylindrical surface of the pellet was covered with a dense gold layer in order to limit side ingress of oxygen. The top surface of the pellet was coated with 215 mg of an oxide-based POX catalyst (HTceramix SA, Switzerland). The latter was mixed with terpineol and ethyl cellulose, and applied as a paste. Air was flushed in the lower compartment and a mixture of methane and argon in the upper one. Oxygen was separated from air by solid-state diffusion through the membrane, and reacted with the methane in the catalyst layer. The extremities of the tubes were sealed in the cold.

Tubular

The design of the tubular reactor is shown in Fig. 2. A ~4-cm-long $La_{0.6}Ca_{0.4}Fe_{0.75}Co_{0.25}O_{3-\delta}$ tube was sealed at both extremities to alumina tube extensions using gold paste. The utility of these extensions is to reduce the thermal gradients along the tube and allow optimal use of its surface for separation. The tube and its extensions were introduced in a coaxial quartz tube (internal diameter: 8 mm). The external surface of the tube was coated with a thin layer of catalyst. In addition, the interstitial space between the separation tube and the quartz tube was filled with a fixed bed of ~1-mm granules coated with the POX catalyst. The choice of this configuration was guided by stability considerations: having the catalyst outside of the tube maintained the tube under compression (more favourable than tension), since both the heat produced on the reaction side and the reducing effect of the fuel produced an expansion of the membrane material. The air flowed inside the tube and the $CH_4 + Ar$ mixture outside in a co-flow way.

Experimental set-up

The global experimental set-up is sketched in Fig. 3. The different gas streams were regulated by mass flow controllers (MFC) (Brooks, Blankhorst) and entered the reactor, which was placed at the centre of a cylindrical furnace (F). In some experiments, the fuel was humidified in a bubbler (B) before entering the reactor. The outlet gas composition was analysed by a gas chromatograph (GC) (Varian) equipped with a 5-Å molecular sieve capillary column (H_2, O_2, N_2, CH_4 and CO) and a Megabore PoraPlot Q capillary column (CO_2). The outlet flux was measured online by a bubble meter (BM). Any leakage could be detected by the presence of N_2 in the reaction product or CO_2 in the outlet air.

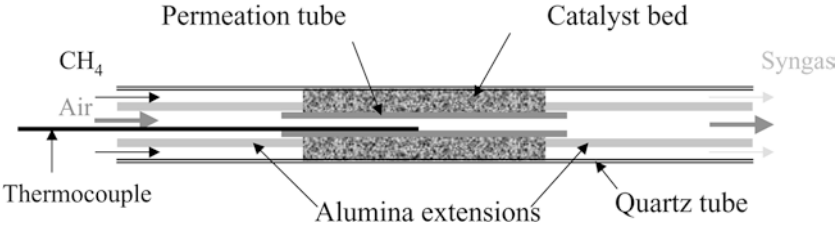

Fig. 2 Tubular reactor design used for the partial oxidation of methane to syngas

Results and discussion

Sample characteristics

The characteristics of the samples used in the different POX reactors are summarised in Table 1. The densities were obtained from Archimedes measurement in isopropanol. Straight 1-m-long tubes could be produced by extrusion, but because of furnace size restrictions, the longest sintered tube was limited to 48 cm. An assortment of dense sintered tubes obtained by extrusion are shown in Fig. 4.

Oxygen permeation fluxes

The permeation fluxes measured through membranes of different thickness in an air/argon pO_2 gradient are shown in Fig. 5 as a function of the inverse temperature. The thinner sample corresponds to a tube of 0.25-mm wall thickness and the thicker sample, to a 1.26-mm-thick pellet. A change in the slope is noticeable around 900 °C for both samples. The values of the related apparent activation energy (E_A) pass from 194 ± 1 ($L = 1.26$ mm) and 151 ± 4 kJ/mol ($L = 0.25$ mm) below 900 °C to 96 and 93 ± 1 kJ/mol, respectively, above 900 °C. Normalised fluxes $L * j_{O_2}$ were calculated by multiplying the permeation flux by the thickness of the membrane, and are reported in the same figure. It is interesting to note that the normalised fluxes of both samples coincide reasonably well (within experimental uncertainty) below 900 °C, but differ above. These features, for this particular pO_2 gradient, can be interpreted as a change of the rate-limiting step with increasing temperature: at lower temperatures (< 900 °C), the oxygen transport through the membranes would be governed by bulk transport ($L * j_{O_2}(0.25\text{ mm}) \cong L * j_{O_2}(1.26\text{ mm})$), whereas at higher temperatures, it would become partially limited by surface or gas-phase reactions ($L * j_{O_2}(0.25\text{ mm}) < L * j_{O_2}(1.26\text{ mm})$). This would also explain the change in the activation energy of the flux. Another possible explanation would be to attribute the discrepancy at high temperature between the normalised fluxes to a reduction of the pO_2 gradient across the membrane due to an increase of the permeation flux. This phenomenon usually results in a gradual inflexion of the flux at high temperatures. However, the difficulty of determining the local value of the pO_2 at the surfaces of the membrane makes any discrimination between these explanations impossible.

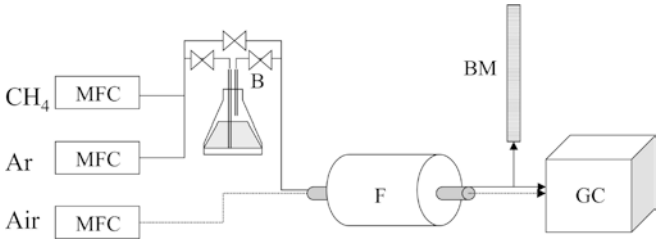

Fig. 3 Experimental set-up used to test the POX reactors. *MFC* mass flow controller, *B* bubbler, *F* furnace, *GC* gas chromatograph, *BM* bubble meter

Table 1 Characteristics of the samples used in the POX- reactor experiments

Sample	Dimensions	Relative density (%)
Diskc-shaped pellet	Diameter: 24 mm Thickness: 1.26 mm	97.2
Tube type 1	Outer diameter: 4.9 mm Wall thickness: 0.5 mm	97.1
Tube type 2	Outer diameter: 5.5 mm Wall thickness: 0.25 mm	97.1

POX reactor performances

The performances of the POX reactors were evaluated on the basis of the outlet gas composition and the conservation equation for each atomic species, assuming no soot formation. The only observed compounds were H_2, H_2O, CO, CO_2, CH_4 and N_2.

The methane conversion was defined by:

$$X_{CH_4} = 1 - \frac{x_{CH_4}}{x_{CH_4} + x_{CO} + x_{CO_2}} \quad (1)$$

where x_i is the molar fraction of species i.

The selectivity for CO was defined by:

$$S_{CO} = \frac{x_{CO}}{x_{CO} + x_{CO_2}} \quad (2)$$

The oxygen permeation flux was

$$j_{O_2} = \frac{F x_{O_2,perm}}{A} \quad (3)$$

where F is the total outlet flux (mol/s) and $A$the surface exchange area (cm^2). The fraction of oxygen that has permeated through the membrane, $x_{O_2,perm}$, was calculated from the atomic balance for C, H and O:

$$\text{C: } x_{CH_{4,in}} = x_{CH_{4,out}} + x_{CO_{2,out}} + x_{CO_{out}} \quad (4)$$

$$\text{H: } 4x_{CH_{4,in}} + 2x_{H_2O_{in}} = 4x_{CH_{4,out}} + 2x_{H_2O_{out}} + 2x_{H_{2,out}} \quad (5)$$

$$\text{O: } 2x_{O_{2,perm}} + x_{H_2O_{in}} + 2x_{O_{2,leak}} = 2x_{O_{2,out}} + 2x_{CO_{2,out}} + x_{CO_{out}} + x_{H_2O_{out}} \quad (6)$$

where the subscript "in" refers to inlet, "out" to outlet, "perm" to the oxygen permeating through the membrane and "leak" to the oxygen originating from air leakage. The latter can be evaluated on the basis of the N_2 content in the outlet gas:

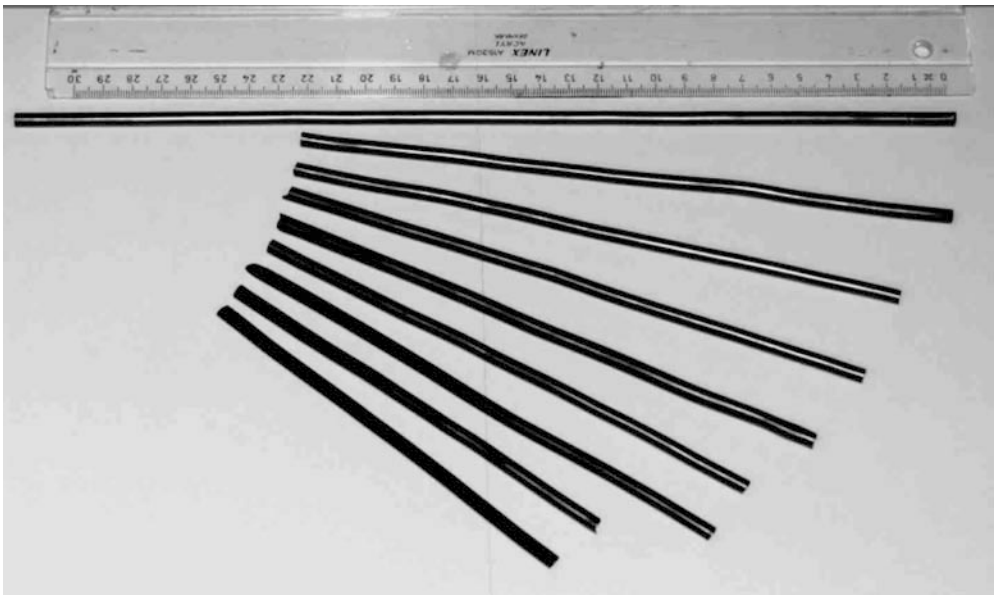

Fig. 4 Assortment of dense sintered $La_{0.6}Ca_{0.4}Fe_{0.75}Co_{0.25}O_{3-\delta}$ tubes obtained by extrusion (length: 15–32 cm)

$$x_{O_{2,leak}} = \frac{0.2096}{0.781} x_{N_{2,out}} \quad (7)$$

where 0.2096 and 0.781 are respectively the fraction of oxygen and nitrogen in air. The contribution of the leakage remained smaller than 1%. Finally, the fraction of oxygen that has permeated through the membrane can be expressed by combining Eqs. 4, 5, 6 and 7:

$$x_{O_{2,perm}} = 2x_{CO_{2,out}} + 1.5x_{CO_{out}} - 0.5x_{H_{2,out}} - \frac{0.2096}{0.781} x_{N_{2,out}}$$

Planar reactor

The catalyst was activated during 15 h at 900 °C with an Ar:CH_4 mixture containing 24% CH_4. After activation, the POX reactor operated for 10 days with variable CH_4 contents in the gas inlet, including 4 days with pure methane, and was finally deliberately stopped. No degradation of the membrane or the catalyst was noticeable for the duration of the experiment.

The effects of the inlet composition on the performances of the POX reactor are shown in Fig. 6. Above 20% CH_4, the selectivity for CO stabilised around 99%, whereas the CH_4 conversion gradually increased up to 60%. This relatively low conversion rate was due to the excess of methane entering the reactor in comparison with the flow of oxygen delivered by the membrane. This is indicated in Fig. 6by the CH_4:O_2 ratio, which systematically exceeded the stoichiometric value of 2 for the POX reaction. In addition, the distance between the inlet tube and the catalyst layer (cf. Fig. 1) was such that a portion of the methane did not transit through the catalyst. This drawback was overcome with the tubular design, as discussed in the next section. Reducing the inlet CH_4 flow from 20 to 15 ml/min enhanced the CH_4 conversion up to 75%. But here again the CH_4:O_2 ratio was ~3 and the measured conversion was in fact close to the maximum conversion attainable with the corresponding ratio. A further reduction of the inlet flux did not improve the conversion but rather decreased the oxygen permeation flux. As expected from the stoichiometry of the POX reaction, the H_2:CO ratio was approximately 2 as shown in Fig. 6. Finally, the oxygen flux across the membrane reached 1.7 μmol/cm^2·s at 918 °C, which is a factor of 30 higher than for the air: argon gradient. The reactor remained stable over 40 h with 99% CO selectivity and 73–75% CH_4 conversion.

Tubular reactor

The performances of the tubular reactor (tube type 1) are shown in Fig. 7. In this case, the methane was humidified in a bubbler before entering the reactor.

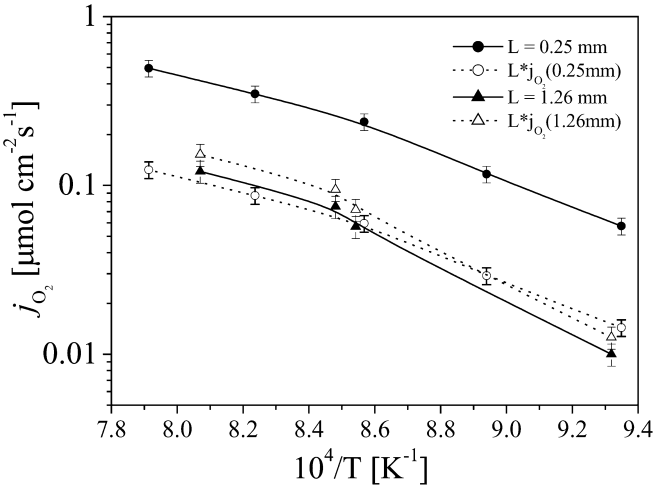

Fig. 5 Arrhenius plot of the oxygen permeation flux across two $La_{0.6}Ca_{0.4}Fe_{0.75}Co_{0.25}O_{3-\delta}$ membranes of different thickness, in an air/argon pO_2gradient: (●) 0.25 mm and (▲) 1.26 mm. Normalised fluxes ($L * j_{O_2}$) are also shown: (○) 0.25 mm and (△) 1.26 mm

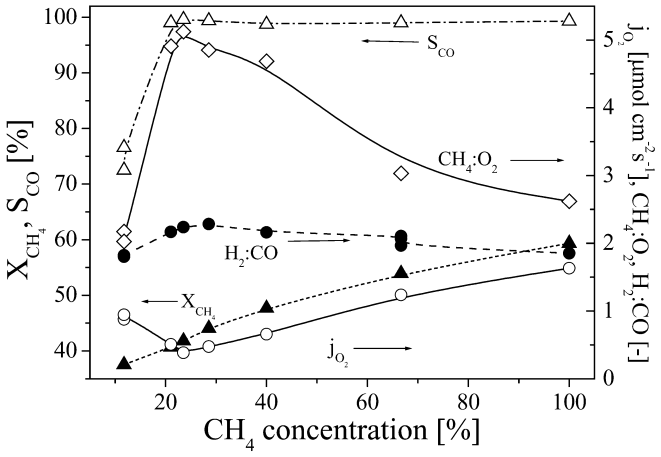

Fig. 6 Catalytic performances of the planar POX reactor as a function of the CH_4 inlet concentration at 918 °C, showing the methane conversion (X_{CH_4}),the CO selectivity (S_{CO}), the oxygen flux (j_{O_2})defined by Eqs. 1, 2 and 3, respectively, and the CH_4:O_2 and H_2:CO ratios. With a $La_{0.6}Ca_{0.4}Fe_{0.75}Co_{0.25}O_{3-\delta}$ pellet (diameter: 24 mm; thickness: 1.26 mm)

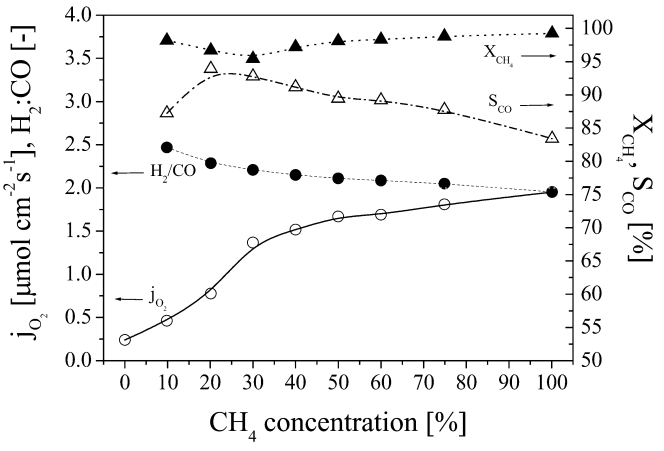

Fig. 7 Catalytic performances of the tubular POX reactor as a function of the CH_4 inlet concentration at 900 °C. With a $La_{0.6}Ca_{0.4}Fe_{0.75}Co_{0.25}O_{3-\delta}$ tube of type 1 (length: 2.2 cm; wall thickness: 0.5 mm). The *notations*are the same as in Fig. 6

The water vapour content was ~3% of the total flow, i.e. the H_2O:CH_4 ratio varied between 30% for tenfold dilution of CH_4 and 3% for pure methane. With the tubular geometry, the methane conversion was much higher since methane was forced to transit through the catalytic bed, reaching 99%. On the other hand, the CO selectivity was reduced to 83% with pure methane. This decrease of the CO selectivity was due to the presence of water vapour that reacts with the CO through the gas shift reaction to form $CO_2$and H_2. Thus, the CO selectivity was improved to 90% when switching to a dry CH_4 inlet. Finally, the H_2:CO ratio exceeded 2 (expected from the stoichiometry of the POX reaction), especially at low CH_4concentrations. This reflects the influence of the high H_2O/CH_4 levels at low CH_4 concentrations that favour steam reforming (H_2:CO = 3).

As in the case of the planar reactor, the oxygen permeation flux across the membrane increased with increasing CH_4content, reaching 2 µmol/cm^2·s with pure methane. In this case, however, the flux was only enhanced by a factor of 8 compared to the air/argon mixture. This could indicate that, in an air/methane gradient, the oxygen permeation flux is not governed by bulk transport but rather surface or gas-phase limitations. There are, however, no sufficient indications to decide whether this limitation occurs on the methane side or the air side, although the latter would be more critical since it would imply the reduction of the membrane material. The different behaviour of the tubular and planar reactors may result from effectively lower local pO_2 gradients, although the pO_2 values calculated from the outlet gas compositions were similar.

A long-term stability test was performed at 900 °C on a similar reactor (tube type 1). Its history is shown in Fig. 8. As the methane content was increased, the oxygen flux gradually reached 2.4 µmol/cm^2·s. However this increase, already described in the previous figure, was compensated by a degradation versus time. The flux finally stabilised around 1.8 µmol/cm^2·s for pure methane. The catalytic properties of the reactor were more stable. The methane conversion (X_{CH_4}) exceeded 95% and the CO selectivity (S_{CO}), 90%. This test was continued over 1,400 h. After 900 h, a small CH_4 leakage appeared after a brief interruption of the air supply. This leakage corresponded initially to 1% of the CH_4 but gradually increased to 6% at the end of the test.

Post-operation examinations

After operation, the membranes were examined by scanning electron (SE) and back-scattered electron (BSE) microscopy. In addition, spot energy-dispersive X-ray (EDX) analysis of the different phases was carried out. However, only preliminary results will be presented since more detailed investigations still have to be undertaken.

A look at the cross-section of the membrane after more than 1,400 h in an air/methane gradient reveals an important alteration of the material. Its stratified aspect is visible in the BSE micrograph presented in Fig. 9. This stratification could be the result of kinetic demixing and decomposition of the material placed in a strong oxygen chemical potential gradient [16]. Delamination of the superficial layers was also observed, probably resulting from the thermal expansion mismatch between the layers during cooling. The approximate compositions of the different surfaces and layers are given in Table 2. The middle portion of the membrane (zone D, ~350 µm thick) consisted of a main dense phase (light) with Ca-enriched clusters (dark). This biphasic texture was also observed in previous work with $La_{0.4}Ca_{0.6}Fe_xCo_{1-x}O_y$ compositions [17]. Although the (La, Ca)

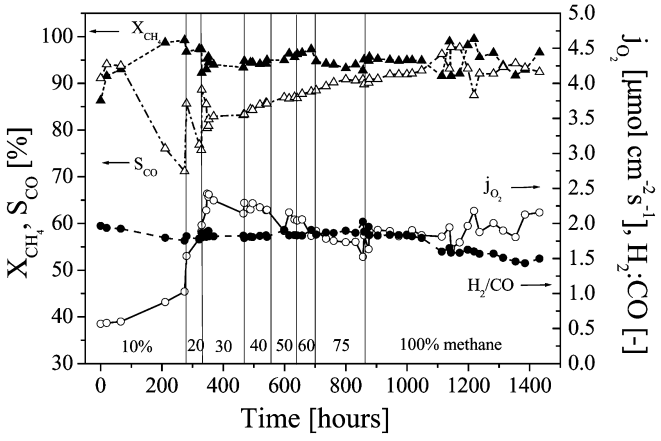

Fig. 8 Catalytic performances of a tubular POX reactor as a function of time over more than 1,400 h. With a $La_{0.6}Ca_{0.4}Fe_{0.75}Co_{0.25}O_{3-\delta}$ tube of type 1 (length: 2.5 cm; wall thickness: 0.5 mm). The *notations*are the same as in Fig. 6

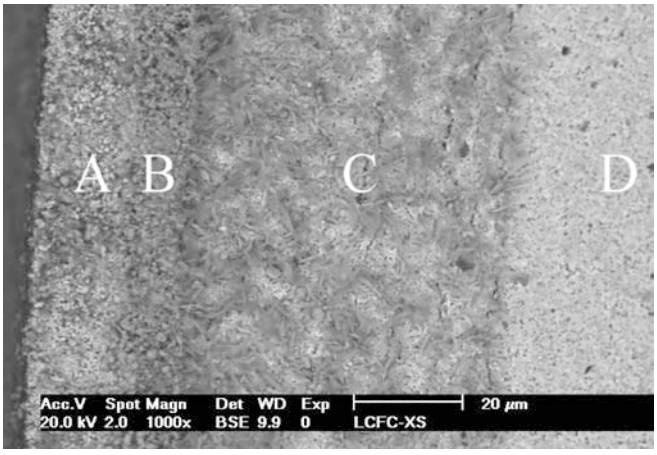

Fig. 9 BSE micrograph of the cross-section of the membrane close to the surface exposed to methane, after >1,400 h operation, showing possible chemical demixing. Refer to Table 2 for the composition of the layers *A* to *D*

composition remained constant over this central zone (D), the main phase was gradually enriched in Co on approaching the air side.

The surface exposed to methane looked porous, as if etched. A global EDX analysis of the surface indicated enrichment in La. Metallic clusters of (Fe, Co) were also observed at the surface. The porous aspect is probably the result of the departure of Ca or local decomposition of the initial membrane material. This porous aspect was also observed in the case of the planar reactor and also in previous work with membranes exposed to an air/H_2 gradient [17].

No evidence of reaction or interdiffusion of compounds between the membrane material and the catalyst was observed. Furthermore, the adhesion of the catalytic layer to the membrane was poor.

The surface exposed to air looked dense and homogeneous. Its composition consisted mainly of Ca and Co with some Fe. Si contamination, probably originating from a silicone glue used for the cold end sealing, was also observed. A look at the cross-section close to the surface shows phase extrusion (Fig. 10). Although the composition of the bulk (light phase, E) remained unchanged ($(La_{0.60}Ca_{0.40})_{1.07}Fe_{0.76}Co_{0.24}O_x$), a second darker phase (F) appeared on the surface, here essentially Co_2O_3.

On the basis of these observations, it was impossible to reach a conclusion on the cause of the eventual failure of the tubular membrane. The air supply incident, mentioned in the previous section, probably created a crack that propagated by creep until final fracture. In fact, after cooling and disjoining, the tube remained in two pieces. On the other hand, the slow degradation of the oxygen flux was probably due to the dramatic compositional and microstructural changes that occurred in the membrane. A more detailed analysis of the membrane combined with a study of the phase stability of $La_{0.6}Ca_{0.4}Fe_{0.75}Co_{0.25}O_{3-\delta}$ will help to identify the cause of failure.

Table 2 Approximate atomic composition of the different demixed layers obtained from local EDX analysis

Zone	Thickness	Composition (%)					Aspect
	(μm)	La	Ca	Fe	Co	O	
CH_4 surface		20.88	1.32	12.27	5.99	59.54	Porous
A	~20						Porous, bi-phasic
		14.29	2.72	21.33	1.55	60.12	Light
		1.93	1.88	19.04	12.23	64.91	Dark
B	~10	0.30	7.09	1.40	30.63	60.58	Porous
C	~60						Porous, bi-phasic
		8.57	9.34	11.16	15.38	55.56	Dark flakes
D	~350						Dense, bi-phasic (CH_4 side)
		15.89	6.01	18.39	0.66	59.04	Light matrix
		9.96	18.67	9.90	0.74	60.73	Dark clusters
		12.00	8.45	15.37	5.97	58.21	Dense (air side)
E	~30	11.37	7.58	13.39	4.20	63.46	Dense
F	~3	0.60	0.84	1.46	36.99	60.11	Dense
Air surface		0.75	12.49	6.13	22.60	57.35	Dense

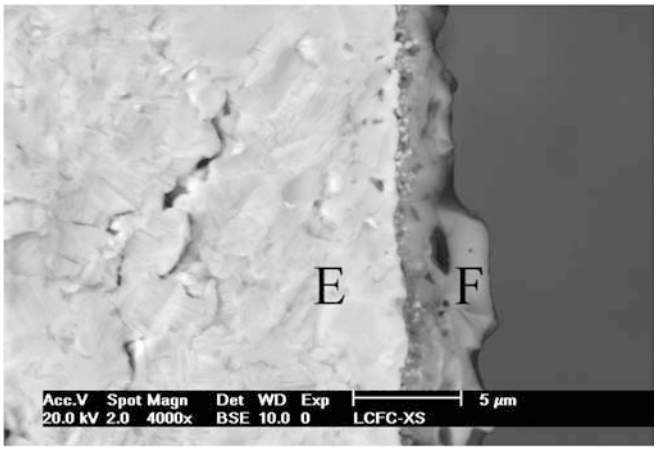

Fig. 10 BSE micrograph of the cross-section of the membrane close to the surface exposed to air, after >1,400 h operation, showing phase extrusion. Refer to Table 2 for the composition of the layers *E* and *F*

Conclusions

$La_{0.6}Ca_{0.4}Fe_{0.75}Co_{0.25}O_{3-\delta}$ membranes were investigated for oxygen separation in POX reactors. Dense, straight and thin-walled (0.5 and 0.25 mm) tubes could successfully be produced by extrusion for this application. Comparison of the oxygen permeation fluxes obtained with two membranes of different thickness in an air/argon pO_2 gradient gave evidence of bulk transport limitation below 900 °C. After adding a POX catalyst to the membranes, catalytic tests were performed with the tubular and planar geometry. A higher CH_4 conversion was reached with the tubular geometry (98% vs. 75%), whereas the tendency was inverted for the CO selectivity (>90% vs. 99%). A tubular POX reactor operated stably over 1,400 h, including >600 h with pure methane in the gas inlet, with >95% conversion and >90% CO selectivity. After operation, the membrane was examined, showing kinetic demixing and decomposition. However, these preliminary results were not sufficient to reach a conclusion on the possible causes of the fracture of the membrane.

Acknowledgements This work was supported by the Swiss Natural Gas Union Funding (FOGA). H. Schindler, from EMPA-Dübendorf, produced the powder.

References

1. Bouwmeester HJM, Burggraaf AJ (1997) Dense ceramic membranes for oxygen separation. In: Gellings PJ, Bouwmeester HJM (eds) The CRC handbook of solid state electrochemistry. CRC, Boca Raton, pp 481–553
2. Wright JD, Copeland RJ (1990) Advanced oxygen separation membrane. Topical report GRI-90/0303, Gas Research Institute
3. Bredesen R, Sogge J (1996) Paper presented at the United Nations Economic Commission for Europe seminar on ecological applications of innovative membrane technology in the chemical industry, Chem/Sem. 21/R.12. Cetaro, Calabria, 1–4 May 1996
4. Hairston D (2002) Chem Eng 7:27
5. Dyer PN, Richards RE, Russek SL, Taylor DM (2000) Solid State Ionics 134:21
6. Balachandran U, Morissette SL, Picciolo JJ, Dusek JT, Poeppel RB, Pei S, Kleefisch MS, Mieville RL, Kobylinski TP, Udovich CA (1992) In: Thompson HA (ed) International gas research conference, vol 2, pp 2499
7. Balachandran U, Dusek JT, Maiya PS, Ma B, Mieville RL, Kleefisch MS, Udovich CA (1997) Catal Today 36:265
8. Tsai LW, Dixon AG, Moser WR, Ma YH (1997) AIChE J 43:2741
9. Sammels AF, Schwarz M, Mackay RA, Barton TF, Peterson DR (2000) Catal Today 56:325
10. Jin W, Li S, Huang P, Xu N, Shi J, Lin YS (2000) J Memb Sci 166:13
11. Ritchie JT, Richardson JT, Luss D (2001) AIChE J 47:2092
12. Wang H, Cong Y, Yang W (2002) J Memb Sci 209:143
13. Pei S, Kleefisch MS, Kobylinski TP, Faber J, Udovich CA, Zhang-McCoy V, Dabrowski B, Balachandran U, Mieville RL, Poeppel RB (1995) Catal Lett 30:201
14. Hendriksen PV, Larsen PH, Mogensen M, Poulsen FW, Wiik K (2000) Catal Today 56:283
15. van Doorn RHE, Bouwmeester HJM, Burggraaf AJ (1998) Solid State Ionics 111:263
16. Schmalzried H, Laqua W (1981) Oxid Met 15:339
17. Diethelm S, Van herle J, Middleton PH, Favrat D (2003) J Power Sources 118:270